Characterization of Clean and Fouled Ultrafiltration Membranes*

J.H. HANEMAAIJER, T. ROBBERTSEN, TH. VAN DEN BOOMGAARD**, C. OLIEMAN, P. BOTH and D.G. SCHMIDT

Netherlands Institute for Dairy Research (NIZO), Ede (The Netherlands)

SUMMARY

Much research into the fundamentals of membrane formation and separation has been performed in order to improve the efficiency of the manufacture of ultrafiltration membranes. Determination of the membrane characteristics is a key problem in these investigations. In this paper, we report on a study of membrane morphology by fractional rejection measurements, using low molecular weight saccharides as the test solute, and by electron microscopy.

Using a simple model for solute/solvent transport through cylindrical pores, a "characteristic pore size" was derived from saccharide rejection data. This pore size of a hypothetical isoporous membrane, interpreting the measured separation characteristics, provides a promising means of describing differences between membranes with respect to pore size and pore size changes caused by solute adsorption.

From high resolution electron micrographs, information was obtained on the skin layer morphologies and, for some membranes the sizes of the larger pores could be estimated.

Keywords: membrane characterization, membrane fouling.

SYMBOLS

C_0 – solute concentration in feed (kg l^{-1})
C – solute concentration in retentate (kg l^{-1})
C_m – solute concentration at membrane surface (kg l^{-1})
C_p – solute concentration in permeate (kg l^{-1})
d_p – pore diameter (nm)

---

d_p^* – characteristic pore diameter (nm)

d_s – solute diameter (nm)

J_v – permeate flow velocity (m s^{-1})

k – mass transfer coefficient (m^2 s^{-1})

K – concentration factor $= V_0/V$ (dimensionless)

R – hydraulic resistance during ultrafiltration or after adsorption (N s m^{-3})

R_m – hydraulic resistance of the membrane (N s m^{-3})

Rej – rejection coefficient (dimensionless)

V – retentate volume (1)

V_0 – feed volume (1)

φ – sieve constant $= C_p/C_m$ (dimensionless)

λ – solute/pore size ratio $= d_s/d_p$ (dimensionless)

Γ – surface concentration of adsorbed solute (mg m^{-2})

INTRODUCTION

The most common route for membrane development is still the adjustment of formation parameters, followed directly by the measurement of separation properties of the cast membrane (Fig. 1). However, in designing ultrafiltration membranes for specific applications, it would be very desirable if, to ensure certain "functional" membrane properties (e.g. flux, rejection) the required membrane characteristics could be defined beforehand and if manufacturing parameters of such membranes were available.

One must be able to understand the processes of membrane formation and the ultrafiltration process (in particular membrane fouling and solute trans-
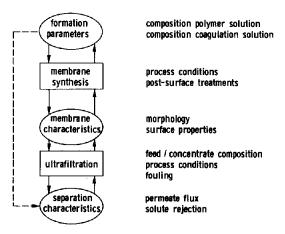

Fig. 1. Membrane design: relations between synthesis and performance.

port mechanisms) in order to meet this goals. One should also be able to actually measure the characteristics of the membrane.

We report on a simple method which provides information on membrane characteristics, and quantifies the degree to which membrane fouling affects these characteristics.

MEMBRANE CHARACTERIZATION METHODS

Membrane characterization has been one of the key areas of recent research in ultrafiltration. Membrane characteristics can be distinguished into morphological properties (pore shape, pore length, pore density and pore size distribution) and into chemical and electrical surface properties. The techniques developed for estimation of pore size distributions can be placed roughly into two groups:

(1) In vitro methods, in which the pore size morphology is determined under non-ultrafiltration conditions (using dry membranes or atypical solvents). Examples are gas adsorption–desorption methods [1–4], thermoporometry [2,6], gas–liquid and liquid–liquid wetting pressure methods [7–9] and electron microscopy [3,10–12].

(2) In vivo methods, in which the separation characteristics are measured under ultrafiltration process conditions, using reference solutes. From rejection data, taking boundary layer (concentration polarization) phenomena into account, the intrinsic membrane sieving properties can be determined. From these data, the membrane pore sizes can be estimated using models for pore morphology and for transport of solutes and solvent through these pores [13–17]. However, common practice is that only rejections for a few reference solutes are measured, using clean membranes, resulting in the so-called molecular weight (mass) cut-off values. An extension of this method, resulting in rejection–molecular mass cut-off curves, is the "fractional rejection" (or "selective permeation") method, in which the test solute has a broad molecular size distribution [2,13,18,19].

Despite the considerable efforts invested in the characterization of ultrafiltration membranes, an easy to use standard method is needed [3,15,20,21]. The growing awareness of the effect of solute–membrane interactions on rejection characteristics [16,22–25] stresses the need for a method which not only characterizes clean membranes but which also quantifies the effects of solute–membrane interactions in the liquids to be processed. This is only possible using rejection-based methods.

REJECTION OF LOW MOLECULAR MASS SACCHARIDES

Rejection measurements using macromolecular test solutes which are almost totally rejected (like dextrans, polyethylene oxides, proteins), suffer from

several problems, mainly related to concentration polarization, unknown solute sizes and solute–membrane interactions. Most of these problems, however, can be reduced by determining only the lower part of the rejection–solute size curve, using low molecular mass saccharides as the test solute mixture, viz.:

Concentration polarization. Because of the low rejection, high diffusivity and low viscosity of the small saccharide molecules, concentration polarization is diminished. Estimation of the mass transfer coefficient k using the Chilton–Colburn and Deissler relationships [26] showed that, for all membranes studied, the solvent flow Jv was larger than k, resulting in a low polarization modulus. Another indication was obtained by the fairly similar permeate fluxes for water with and without saccharides. The impact is that intrinsic rejection can be measured directly, avoiding inaccuracies in the descriptions of the mass transfer in the boundary layer.

Solute size and conformation. Solute sizes are relatively well-defined; deformability is small compared to such compounds as dextrans.

Interactions. The influence of solute–solute and solute–membrane interactions on the rejection measurements is small, as will be demonstrated. This also creates possibilities for measurement of changes in pore size, caused by membrane fouling.

Analysis. Efficient chromatographic analysis of retentates and permeates is possible.

Even very small saccharides are rejected by rather open ultrafiltration membranes after membrane fouling, as is illustrated in Table I. Fouling due to adsorption of proteins (in this case a 3:1 mixture of β-lactoglobulin and α-lactalbumin) is known to be strongest near the iso-electric point of the protein [27]; therefore, at pH 5, more protein can be expected to be adsorbed. This results in an increased rejection of saccharide molecules.

Another illustration of the effect of membrane fouling on separation characteristics is given in Fig. 2. It is clearly demonstrated that, during ultrafiltra-

TABLE I

Effect of protein adsorption on the rejection of some saccharides
Membrane: acrylic copolymer, cut-off 30 000 dalton, $T=50°C$

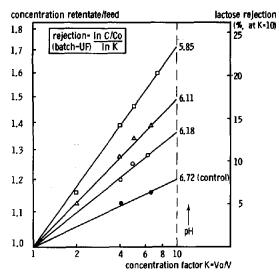| Membrane pretreatment	pH buffer solution	Rejection (%)		
		Glucose	Lactose	Raffinose
None	6.6	1	1	1
(cleaned)	5.0	1	1	0
Adsorption of	6.6	2	3	3
whey proteins	5.0	3	11	18

Fig. 2. Effect of pH on lactose rejection during batch ultrafiltration of fermented skim milk, Abcor UF pilot plant, 30 m²; HFK–131 membranes; $T_{UF} = 50°C$.

TABLE II

Rejection of glucose (S1) by a whey protein-pretreated membrane (polysulfone, cut-off 20 000 dalton), using several saccharide blends

Test solution-sequence:	S1→	S1−S20→	S1→	S1+S3→	S1
S1 rejection (%):	3	3	4	3	3
S10 rejection (%)		42			

tion of milk, the lactose content of the retentate increases as the pH decreases, thus protein fouling is higher. This membrane showed no lactose rejection for solutions without proteins.

In several experiments, it has been confirmed that saccharide–solute and saccharide–membrane interactions do not significantly affect the measurements. For instance, Table II shows that glucose (S1) rejection (in a sequence of experiments) is unaffected by the presence of higher molecular mass saccharides; this membrane was brought into contact with a whey protein mixture, at pH 5.0. The same was observed for clean membranes, suggesting a negligible influence of saccharide–membrane and saccharide–adsorbed protein interactions on the saccharide rejection measurements.

EXPERIMENTAL

Saccharide test solute mixture

The mixture of low molecular mass saccharides was prepared by mixing several starch hydrolysates and by subsequently removing the high molecular mass saccharides (by ultrafiltration) and part of the glucose (by nanofiltration).

For characterization of the mixture and analysis of retentates and permeates, a high-performance liquid chromatographic (HPLC) method was developed, with the potential to quantify up to 11 glucose units – saccharides (Fig. 3). The HPLC was performed with two Biorad HPX 42 A columns connected in series; the eluant was water, 0.3 ml min^{-1}, at 75°C; detection was performed by refractive index measurement at 40°C.

The hydrodynamic size of the saccharides was estimated by several methods [28]:
- molar volumes (densities) of glucose, maltose, raffinose
- conformational statistics (theoretical radii of gyration)
- Stokes–Einstein diffusion coefficients and intrinsic viscosities
- Stuart models
- HPLC elution times

β-Lactoglobulin

β-Lactoglobulin genetic variants A and B (used as a mixture) and α-lactalbumin were isolated from desalted, clarified casein whey by ion-exchange chro-
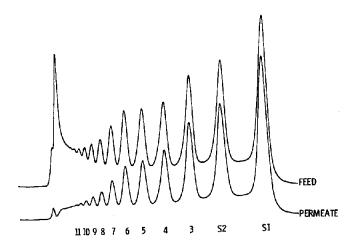

Fig. 3. Typical HPLC pattern of feed and permeate resulting from characterization of an UF membrane using a saccharide mixture.

matography (Pharmacia Stack KS 370/15, DEAE Sepharose Fast Flow Anion Exchanger).

Water

Demineralized water was prefiltered before use by reverse osmosis (Osmonics PA 99 RO-module).

Membranes

The membranes used are summarized in Table III.

Ultrafiltration equipment

The adsorption and permeation experiments were performed in laboratory X-flow equipment, a picture of which is shown in Fig. 4. Four modules (each containing 40 cm^2 of membrane surface) could be operated in parallel. Each experiment was performed at 50°C, which is a common process temperature in ultrafiltration. Other experimental conditions were aimed at diminishing of concentration polarization (pressure 50–100 kPa, X-flow velocity, 1 m s^{-1}).

Electron microscopy

Electron micrographs of the surface and cross-section of various membranes were obtained using a JEOL JEM 1200 EX high resolution scanning–transmission electron microscope. For gold coating of the samples a Balzer MED 10 evaporation unit was used.

TABLE III

Data for various membranes used in this study

Code	Material	Molecular mass cut-off value[a] (daltons)	Surface character
PSf50^{000}	polysulfone	50 000	hydrophobic
PSf20^{000}	polysulfone	20 000	hydrophobic
PSf6^{000}	polysulfone	6 000	hydrophobic
RC30^{000}	regenerated cellulose	30 000	hydrophilic
RC5^{000}	regenerated cellulose	5 000	hydrophilic
AC30^{000}	acrylic copolymer	30 000	hydrophilic

[a]According to the suppliers

Fig. 4. Laboratory X-flow equipment of simultaneous studying of four UF/MF membranes.

RESULTS AND DISCUSSION

Saccharide rejections for clean and fouled membranes

The usefulness of the method was demonstrated by rejection experiments with five ultrafiltration membranes having different surface properties and cut-off values. Results, including the effect of membrane fouling on the separation charcteristics, are shown in Fig. 5. In Fig. 5A it can be seen that cut-off values (as given by the manufacturers) do not run parallel to the saccharide rejections observed: note the large difference in rejection between the membranes with 5000 and 6000 cut-off values. This again illustrates the dependence of cut-off data on test conditions and test solutes.

Fig. 5B shows the rejections measured after the membranes had been brought into contact with a buffered protein solution. Rejections of the hydrophobic (PSf) membranes increase sharply; those of the hydrophilic (RC) types do not change significantly.

This increase in rejection, caused by protein adsorption, runs parallel to an
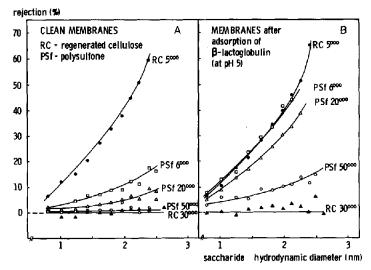
rejection (%)

Fig. 5. Rejection of oligosaccharides by several commercial hydrophobic and hydrophilic ultrafiltration membranes. Effect of protein adsorption.
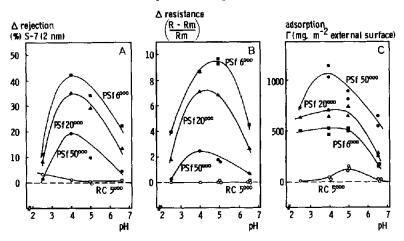

Fig. 6. Influence of adsorption of β-lactoglobulin from solutions of different pH onto membranes of different surface characteristics and pore size on the rejection of saccharides and on the hydraulic resistance.

increase in hydraulic resistance (decrease in hydraulic permeability) for all membranes, as is shown in Figs. 6A and 6B. Increases in rejection (of a saccharide of about 2 nm size) and resistance are largest around pH 4, which is near the point of minimal stability (pH 4.5) of β-lactoglobulin [29]. Also, increases are largest for the polysulfone membrane with the lowest cut-off value. This is understandable from the view that protein adsorption decreases the

pore size; at a given thickness of adsorbed protein layers, it is particularly the small pore membranes that are affected.

In the above experiments, the amounts of adsorbed protein were also determined after desorption by means of a SDS detergent solution; removal was such that the water permeability of the membranes was restored. Results are shown in Fig. 6C. The large amounts of protein recovered from the hydrophobic polysulfone membranes present another indication that the location of adsorption is primarily inside the membrane. An explanation for the lower adsorption onto membranes with smaller cut-off values might be found in the smaller pore surface area, and, of course, in the higher protein rejection of the "tighter" membranes.

Pore size estimation based on rejection measurements

The exact pore size distribution cannot be derived from rejection data without exact information on the morphology (pore shape, pore length, pore density etc.) of the membrane skin layer, or without knowledge of the mechanisms of solute and solvent transport through these pores. As long as this information is not sufficiently available, one has to resort to the application of models in order to relate rejections to pore size. One of the earliest and most frequently used models is that described by Ferry [5], shown in Fig. 7. This model accounts for the partitioning of solutes in the pore entrance area of cylindrical
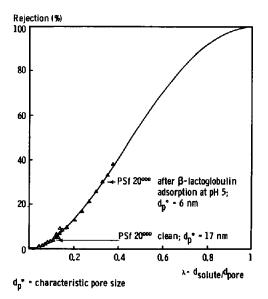

Fig. 7. Theoretical rejection curve for steric rejection of a non-adsorbing sphere by a cylindrical pore (according to Ferry [5]) and some experimental saccharide values.

pores, and is based on the fact that the centre of a solute molecule cannot approach the pore wall closer than the radius of the molecule.

This consideration leads to the following relation for the sieve constant φ (the ratio between the permeate concentration C_p and concentration at the membrane surface C_m):

$$\varphi = 2\left(1 - \frac{d_s}{d_p}\right)^2 - \left(1 - \frac{d_s}{d_p}\right)^4 \tag{1}$$

in which d_s and d_p are the diameter of solute and pore, respectively. With $\lambda = d_s/d_p$ [13] this yields for the rejection:

$$Rej = 1 - \varphi = [\lambda(\lambda - 2)]^2 \tag{2}$$

Attempts to describe the measured rejections by assuming an isoporous membrane using this simple model were surprisingly successful. Two examples are given in Fig. 7.

Without pretending that an exact physical value is given, this pore size d_p^* of an imaginary isoporous membrane, interpreting the measured rejections, could be regarded as a membrane characteristic; in particular because it seems not to be influenced by the solute size to any great extent (which is in accordance with expectations based on cylindrical pores, the Ferry model for solute partitioning and Poiseuille solvent flow).
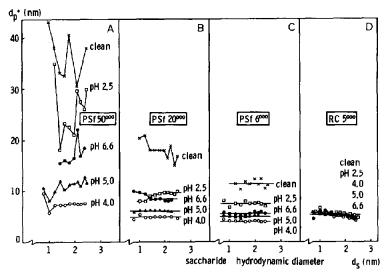

Fig. 8. Characteristic pore size of several ultrafiltration membranes before and after adsorption of β-lactoglobulin (at different pH values), determined by oligosaccharide rejection.

104

TABLE IV

Characteristic pore size of several ultrafiltration membranes before and after protein adsorption, determined by rejection of ligosaccharides

membrane	Characteristic pore diameter (nm)				
	Clean membrane	After β-lactoglobulin adsorption			
		pH 6.6	pH 5.0	pH 4.0	pH 2.5
PSf50^{000}	33 –38	16 –17	9 –12	7.5	20 –30
PSf20^{000}	17 –18	8 –10	6	5	8 –10
PSf6^{000}	11 –12	5.5	5	4	7.5
RC5^{000}	4.5- 6	4.5- 6	4.5- 6	4.5-6	5 – 6
RC30^{000}	35 –45		20 –30		

In Fig. 8 these "isoporous characteristics – sizes", directly derived from saccharide rejection data, are given for four different membranes. Several conclusions can be drawn from this figure:

(1) The effect of solute size on the characteristic pore sizes seems limited.

(2) Membrane fouling caused by protein adsorption can be quantified in terms of pore narrowing using this method.

(3) Differences in rejection characteristics between various membranes may be strongly reduced after protein adsorption.

(4) For the hydrophilic, low protein adsorbing RC5^{000} membrane, the calculated pore sizes are not affected by protein adsorption.

The characteristic pore size data are summarized in Table IV.

Pore size estimation using electron microscopy

In order to obtain insight into the physical significance of the "characteristic pore size", an attempt was made to visualize skin layer morphology and pores of the ultrafiltration membranes by using high resolution scanning electron microscopy (SEM).

The micrographs in Fig. 9 show cross-sections of the PSf20^{000} membrane, obtained at magnifications of 1000, 10 000 and 50 000. This membrane shows a rather open, coral-like substructure. Also, the skin layer seems much thinner than is usually assumed (e.g. ref. 30); thickness appears to be about 100 nm. The same morphology was found for the PSf6^{000} and PSf5^{000} membranes.

Membranes manufactured from other polymers by immersion precipitation can have a clearly different morphology, as is illustrated in Fig. 10, which shows cross-sections of a membrane made out of charged acrylic copolymer. These

micrographs were obtained at magnifications of 1200, 25 000 and 100 000. This membrane has a denser, more packed bed like substructure, and a thicker skin (more than 500 nm). The dark lines, visible in the skin layer between the nodules, could indicate pores.

Figs. 11, 12 and 13 show micrographs of the surfaces of the PSf6^{000}, PSf20^{000} and PSf50^{000} membranes, obtained at a magnification of 100 000. The latter was also examined at a magnification of 200 000. Circular pore openings are visible in the PSf20^{000} and the PSf50^{000} membranes. Because skin thickness was shown to be rather small, it can be expected that the size of the pores in

Fig. 9. Electron micrographs of the cross-section of a polysulfone ultrafiltration membrane with 20 000 dalton cut-off.

Fig. 10. Electron micrographs of the cross section of an acrylic ultrafiltration membrane with 30 000 dalton cut-off.
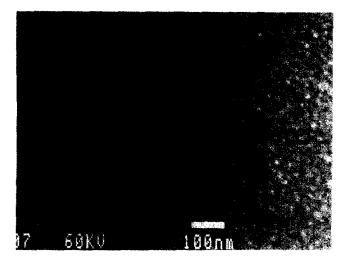
Fig. 11. Electron micrograph of the surface of a polysulfone membrane with 6 000 dalton cut-off.

Fig. 12. Electron micrograph of the surfce of a polysulfone membrane with 20 000 dalton cut-off.

the membrane does not differ much from that of the pore openings at the surface. Taking the thickness of the gold coating (approximately 5 nm) into account, it may be argued (with the necessary reservations) that the $PSf20^{000}$ membrane contains pores with a size up to approximately 25 nm, and the $PSf50^{000}$ type up to approximately 50 nm.

Because the characteristic pore sizes derived from saccharide rejection data strongly depend on the larger pores (as does the solvent–solute transport), these pore sizes do not seem unrealistic.
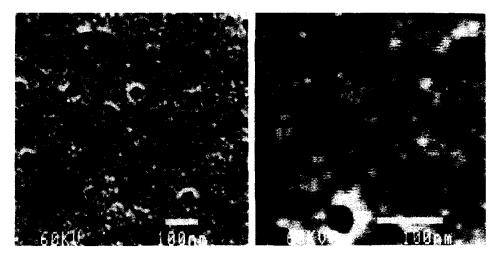
Fig. 13. Electron micrographs of the surface of a polysulfone membrane with 50 000 dalton cut-off.

CONCLUSION

The aims of ultrafiltration applications are:
– to achieve a good separation between macromolecular solutes (often proteins) and smaller molecules (water, salts, saccharides)
– to maintain a high permeate flux.

It is obvious that, for complex process streams, the best results are not necessarily obtained by using the membrane with the most promising water permeability and rejections, measured for model solutes. It is our view that the method described above presents an improved and practical way to obtain information on which type of membrane should be used for a specific separation. It allows the study of intrinsic separation characteristics and permeability of membranes (having different structural and chemical characteristics) not only in the clean state, but also application-directed, in that the saccharide mixture is added to the liquid to be processed. And, as long as membrane morphology has not been revealed accurately enough to produce a satisfactory description of solute–solvent transport through pores, the "characteristic pore size" derived from low molecular weight saccharide rejection data could provide a pragmatic tool in the characterization of clean and fouled ultrafiltration membranes and, hence, in membrane design.

ACKNOWLEDGEMENTS

authors would also like to acknowledge the assistance of C. de Graaf, R. Holleman, J. Leenders and D. Romijn.

REFERENCES

1   M. Bodzek, Pol. J. Chem., 57 (1983) 919.
2   C.A. Smolders and E. Vugteveen, Polym. Mat. Sci. Eng., 50 (1984) 177.
3   L.J. Zeman and G. Tkacik, Polym. Mat. Sci. Eng., 50 (1984) 169.
4   D. Bhattacharrya, M. Jevtitch, J.T. Schrodt and G. Fairweather, Chem. Eng. Commun., 42 (1986) 111.
5   J.D. Ferry, Chem. Rev., 18 (1936) 373.
6   C. Eyraud, Paper presented at Summer School on Membr. Sci. Technol., Cadarache, France, Sept. 3-7 (1984).
7   F.W. Altena, H.A.M. Knoef, H. Heskamp, D. Bargeman and C.A. Smolders, J. Membr. Sci., 12 (1983) 313.
8   S. Munari, A. Bottino, G. Capannelli and P. Moretti, Desalination, 53 (1985) 11.
9   M.G. Katz and G. Baruch, Desalination, 58 (1986) 199.
10 U. Merin and M. Cheryan, J. Appl. Polym. Sci., 25 (1980) 2139.
11 A.G. Fane, C.J.D. Fell and A.G. Waters, J. Membr. Sci., 9 (1981) 245.
12 W. Pusch and A. Walch, J. Membr. Sci., 10 (1982) 325.
13 L.J. Zeman and M. Wales, Sep. Sci. Technol., 16 (1981) 275.
14 S. Nakao and S. Kimura, J. Chem. Eng. Japan, 15 (1982) 200.
15 C.R. Robertson, Molecular and macromolecular sieving by asymmetric ultrafiltration membranes, OWRT report PB 85-157766, Stanford Univ., USA, Sept. 1984.
16 B.D. Mitchell and W.M. Deen, J. Membr. Sci., 19 (1984) 75.
17 G. Jonsson, Desalination, 53 (1985) 3.
18 A.N. Cherkasov, A.E. Polotskii, L. Yu. Goreleva, V.P. Zhemkov and B.G. Belenkii, Kolloidh. Zh., 43 (1981) 661.
19 J. Kasotis, J. Schmidt, L.T. Hodgins and H.P. Gregor, J. Membr. Sci., 22 (1985) 61.
20 G. Trägard, Desalination, 53 (1985) 25.
21 G. Trägard and K. Ölund, Desalination, 58 (1986) 187.
22 J.S. Schultz, R. Valentine and Ch.Y. Choi, J. Gen. Physiol., 73 (1979) 49.
23 L.J. Zeman, J. Membr. Sci., 15 (1983) 213.
24 H. Reihanian, C.R. Robertson and A.S. Michaels, J. Membr. Sci., 16 (1983) 237.
25 A.G. Fane, C.J.D. Fell and K.J. Kim, Desalination, 53 (1985) 37.
26 G. Jonsson and C.E. Boesen, Polarization phenomena in membrane processes in: G. Belfort (Ed.), Synthetic Membrane Processes, Academic Press, New York, (19983).
27 W. Norde, Physicochemical aspects of the behaviour of biological components at solid/liquid interfaces, Symposium Microspheres and Drug Therapy, Amsterdam, Oct. 30-Nov. 6 (1983).
28 Th. van den Boomgaard, NIZO-Report NOV-1151 (1986).
29 R. Townend and S.N. Timasheff, J. Am. Chem. Soc., 82 (1960) 3168.
30 H. Strathmann, Trennung von molekularen Mischungen mit Hilfe synthetischer Membranen, Steinkopf Verlag, Darmstadt (1979).